© 2016. Published by The Company of Biologists Ltd | Journal of Cell Science (2016) 129, 1101-1114 doi:10.1242/jcs.179663

RESEARCH ARTICLE

SHIP2 controls plasma membrane PI(4,5)P2 thereby participating in the control of cell migration in 1321 N1 glioblastoma cells

William's Elong Edimo[1], Somadri Ghosh[1], Rita Derua[2], Veerle Janssens[2], Etienne Waelkens[2], Jean-Marie Vanderwinden[3], Pierre Robe[4] and Christophe Erneux[1,*]

ABSTRACT

Phosphoinositides, particularly phosphatidylinositol (3,4,5)-trisphosphate [PI(3,4,5)P3] and phosphatidylinositol 4,5-bisphosphate [PI(4,5)P2], are recognized by SHIP2 (also known as INPPL1) a member of the inositol polyphosphate 5-phosphatase family. SHIP2 dephosphorylates PI(3,4,5)P3 to form PI(3,4)P2; the latter interacts with specific target proteins (e.g. lamellipodin). Although the preferred SHIP2 substrate is PI(3,4,5)P3, PI(4,5)P2 can also be dephosphorylated by this enzyme to phosphatidylinositol 4-phosphate (PI4P). Through depletion of SHIP2 in the glioblastoma cell line 1321 N1, we show that SHIP2 inhibits cell migration. In different glioblastoma cell lines and primary cultures, SHIP2 staining at the plasma membrane partly overlaps with PI(4,5)P2 immunoreactivity. PI(4,5)P2 was upregulated in SHIP2-deficient N1 cells as compared to control cells; in contrast, PI4P was very much decreased in SHIP2-deficient cells. Therefore, SHIP2 controls both PI(3,4,5)P3 and PI(4,5)P2 levels in intact cells. In 1321 N1 cells, the PI(4,5)P2-binding protein myosin-1c was identified as a new interactor of SHIP2. Regulation of PI(4,5)P2 and PI4P content by SHIP2 controls 1321 N1 cell migration through the organization of focal adhesions. Thus, our results reveal a new role of SHIP2 in the control of PI(4,5)P2, PI4P and cell migration in PTEN-deficient glioblastoma 1321 N1 cells.

KEY WORDS: SHIP2, Phosphoinositide, Cell migration, Focal adhesion

INTRODUCTION

Phosphoinositides play a central role in many physiological mechanisms allowing the recruitment of signaling proteins to membranes through specific phosphoinositide-binding motifs (Balla, 2013). Phosphoinositide 3-kinase (PI3K) and PTEN are major positive and negative regulators, respectively, of the pathway, which regulates cell growth, survival, proliferation and motility (Chalhoub and Baker, 2009). These key signaling enzymes are two of the most frequently mutated proteins in human cancers, particularly in glioblastoma (Song et al., 2012). Two distinct pathways control the dephosphorylation of phosphatidylinositol (3,4,5)-trisphosphate [PI(3,4,5)P3]: the 3-phosphatase reaction mediated by the tumor suppressor PTEN and several inositol polyphosphate 5-phosphatases (Balla, 2013; Pirruccello and De Camilli, 2012). There are ten different enzymes that often catalyze the dephosphorylation of both phosphatidylinositol (4,5)-bisphosphate [PI(4,5)P2] and [PI(3,4,5)P3] at the 5-position, although it is not always clear whether or not both lipids are modified in intact cells. Despite some sequence identity in their catalytic sites, it appears that inositol polyphosphate 5-phosphatases are not redundant in intact cells and mutations of several members of this family have been found to be associated with very specific human diseases such as the Lowe syndrome, Dent disease and Joubert syndrome (Balla, 2013; Billcliff and Lowe, 2014; Pirruccello and De Camilli, 2012; Staiano et al., 2015). Recent data have clearly shown the tumor regulatory role of the inositol polyphosphate 5-phosphatases in different type of cancers such as glioblastoma (Kim et al., 2014). In breast cancer cells, the inositol polyphosphate 5-phosphatase synaptojanin 2 promotes cell migration and invasion in culture but also lung metastasis of breast tumor xenografts in mice (Ben-Chetrit et al., 2015). In another study, depletion of the proline-rich inositol polyphosphate 5-phosphatase PIPP (also known as INPP5J) has been shown to increase transformation and accelerate oncogene-driven tumor growth *in vivo*, whereas paradoxically reducing cell migration, invasion and metastasis (Ooms et al., 2015); this study identifies PIPP as a suppressor of oncogenic PI3K signaling in breast cancer.

The Src homology 2 (SH2)-domain-containing inositol phosphatase 2 (SHIP2, also known as INPPL1) is another member of the inositol polyphosphate 5-phosphatase family that recognizes a series of phosphoinositides, particularly PtdIns(3,4,5)P3, as substrate. It has been reported that SHIP2 is overexpressed in a series of human cancers, e.g. in breast cancer cells where its overexpression correlates with shorter survival (Prasad et al., 2008b). In other cells, it is presented as a tumor suppressor, e.g. in squamous cell carcinoma or glioblastoma (Elong Edimo et al., 2011; Yu et al., 2008). SHIP2 also regulates important biological mechanisms such as cell adhesion (Prasad et al., 2002), migration (Yu et al., 2010) or endocytosis at the leading edge of the cells (Boucrot et al., 2015). It is accepted that PI(3,4,5)P3 is the main SHIP2 substrate (Giuriato et al., 2002; Nakatsu et al., 2010; Taylor et al., 2000) and its reaction product phosphatidylinositol 3,4-bisphosphate [PI(3,4)P2] is a lipid involved in endocytosis, lamellipodia formation (Krause and Gautreau, 2014), invadopodium maturation (Sharma et al., 2013) and ruffle formation (Hasegawa et al., 2011). In addition to PI(3,4,5)P3, PI(4,5)P2 is also a substrate of SHIP2 although evidence of this in intact cells has been more difficult to establish, although it has been observed in a very few models, e.g. in COS-7 cells (Nakatsu et al., 2010). In COS-7 cells, SHIP2 associates at clathrin-coated pits at the early stages of their formation. By the use of a small interfering RNA (siRNA) approach for SHIP2, it has been proposed that both the substrates PI(4,5)P2 and PI(3,4,5)P3 have a positive role on coat assembly (Nakatsu et al., 2010). In other cell

[1]IRIBHM, Campus Erasme, ULB Bâtiment C, 808 route de Lennik, Bruxelles B-1070, Belgium. [2]Protein Phosphorylation & Proteomics Lab, Department of Cellular and Molecular Medicine, Faculty of Medicine, KU Leuven, Herestraat 49 PO-box 901, Leuven B-3000, Belgium. [3]Laboratory of Neurophysiology, ULB Bâtiment C, 808 route de Lennik, Bruxelles B-1070, Belgium. [4]Génétique Humaine, GIGA center, Ulg, B-4000 Belgium.

*Author for correspondence (cerneux@ulb.ac.be)

Received 27 August 2015; Accepted 25 January 2016

Journal of Cell Science (2016) 129, 1101-1114 doi:10.1242/jcs.179663

contexts, this is not observed; for example, in mouse embryonic fibroblasts the amount of PI(4,5)P2 determined by [^{32}P] labeling was not significantly different between SHIP2$^{+/+}$ and SHIP2$^{-/-}$ fibroblasts (Blero et al., 2005). This was estimated in a global cell population starting from a relatively large amount of cells (1.5×10^6 cells) either in unstimulated or serum stimulated cells.

Here, we specifically aimed to image the different phosphoinositides at the plasma membrane in human glioblastoma cell lines and primary cultures. As PTEN is one of the most mutated genes in glioblastoma (Westhoff et al., 2014), we have chosen to quantify the phosphoinositides in PTEN-null glioblastoma 1321 N1 cells (hereafter N1 cells). In this model, SHIP2-depleted cells migrate faster, concomitantly with PI(4,5)P2 upregulation and phosphatidylinositol 4-monophosphate (PI4P) downregulation at the plasma membrane. This controls cell migration through affecting the organization of focal adhesions. Our results thus reveal a new role of SHIP2 in the control of PI(4,5)P2, PI4P and cell migration in PTEN-deficient glioblastoma.

RESULTS

Lowering SHIP2 expression potentiated cell migration in N1 glioblastoma cells

We used a PTEN-deficient glioblastoma cell line (N1 cells) to generate cell lines where SHIP2 was depleted by short hairpin RNA (referred to as N1shSHIP2 cells) (Elong Edimo et al., 2011). These cells show a more than 95% reduction in SHIP2 as seen by western blotting using either antibodies against SHIP2 or against SHIP2 phosphorylated at S132 (pSHIP2 S132) (Fig. 1A). PI(3,4,5)P3 (the

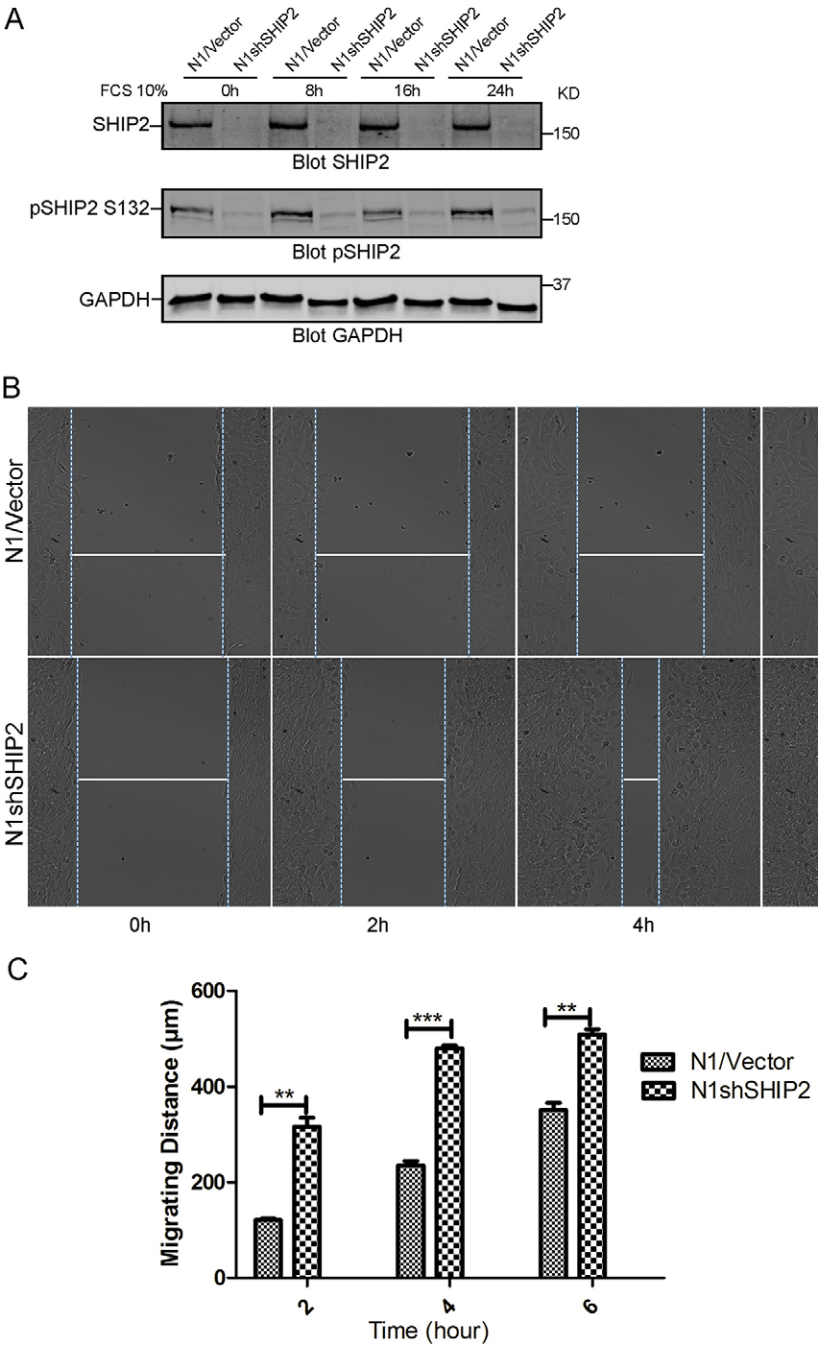

Fig. 1. SHIP2-depleted N1 cells show an increase in cell migration as compared to vector control cells. (A) Western blot analysis of SHIP2 and pSHIP2 S132 expression in vector control (N1/Vector) and N1shSHIP2 cells unstimulated or stimulated with 10% FCS. (B) Negative control of SHIP2 on cell migration assessed by a scratch wound assay. Phase-contrast microscopy images were taken at 0, 2, 4, 6 h of migration. Scale bar: 75 µm. (C) Migration distances of cells shown after 2, 4 and 6 h of migration (mean± s.e.m. of five determinations for each condition in three independent experiments). $^{**}P<0.01$; $^{***}P<0.001$ (two-way ANOVA followed by Bonferroni post-test).

Journal of Cell Science

Journal of Cell Science (2016) 129, 1101-1114 doi:10.1242/jcs.179663

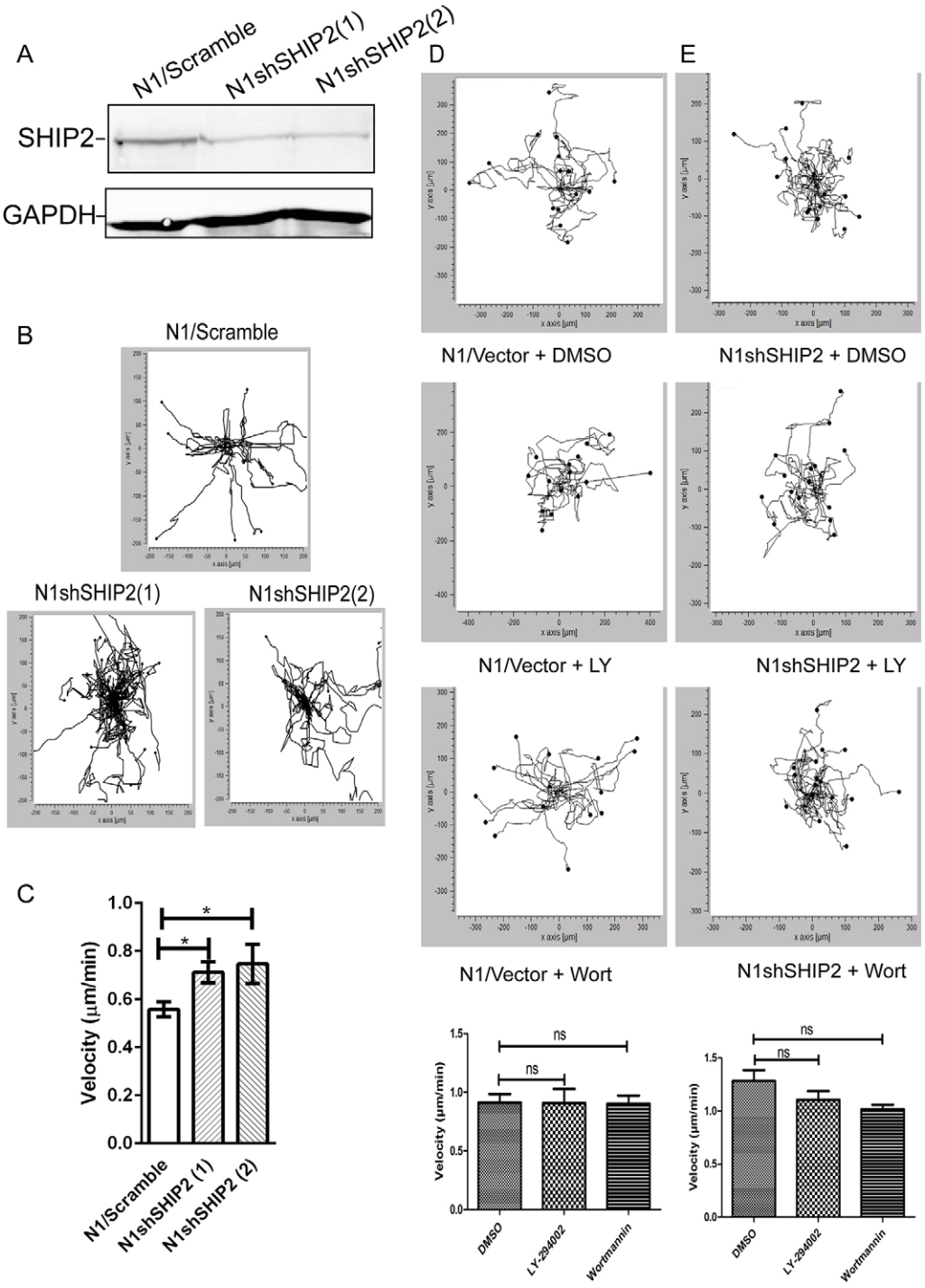

Fig. 2. The effect of PI3K inhibitors on cell migration in control and SHIP2-depleted N1 cells. (A) Western blot analysis of SHIP2 and GAPDH in total cell lysates of N1 cells expressing scrambled shRNA (N1/Scramble) or one of two SHIP shRNAs [N1shSHIP2(1) or N1shSHIP2(2)] maintained in 10% serum. (B) The respective cells were tracked over time using chemotaxis and migration software from Ibidi and depicted as the ratio of axial (*y*-axis) to tangential (*x*-axis) motility. (C) Cell velocity over three independent experiments is graphically depicted as mean±s.e.m. In each experiment, 25 representative cells were followed for each condition. **P*<0.05 (Student's *t*-test for unpaired data followed by a Mann–Whitney test). (D,E) Effect of PI3K inhibitors. Wort, wortmannin; LY, LY-294002. N1/Vector, vector control cells. The data were obtained in three independent experiments. Cell velocity is expressed as mean±s.e.m. *P*>0.05 for the cells treated with inhibitors as compared with the DMSO control (ns).

main SHIP2 substrate; Blero et al., 2001, 2005) was upregulated in N1shSHIP2 cells as compared to vector-transfected (or control) cells, as expected for a PI(3,4,5)P3 phosphatase (Elong Edimo et al., 2011). This had a positive impact on the level of Akt phosphorylated at S473 and T308 (pAkt S473/T308) (Fig. S1A) and cell proliferation (Elong Edimo et al., 2011). As SHIP2 interacts with cytoskeletal proteins (Dyson et al., 2001), we now asked whether cell migration would also be affected in SHIP2-depleted cells as compared to control cells. We used a scratch wound healing assay and live-cell imaging to answer this question. As measured within 6 hours of migration, cell migration was significantly increased in SHIP2-deficient cells as compared to vector-transfected cells. This could be seen both in the absence and presence of serum (Fig. 1B,C; Movie 1). We confirmed this result using two different human SHIP2-targeting shRNAs obtained from the Sigma MISSION library: migration was also increased in SHIP2-depleted cells [N1shSHIP2(1) or N1shSHIP2(2) cells as compared to N1/Scramble, Fig. 2A–C]. Addition of the PI3K inhibitors LY-294002 or wortmannin for 30 min completely abolished the production of PI(3,4,5)P3 in N1 or N1shSHIP2 cells (Elong Edimo et al., 2011). In contrast, cell migration was not influenced by the presence of the PI3K inhibitors both in N1 vector control and N1shSHIP2 cells. This was observed both by live-cell imaging of individual cells, to determine the speed of migration (Fig. 2D,E) or in a scratch wound healing assay (Fig. S2A,B). This suggests that in N1

Journal of Cell Science (2016) 129, 1101-1114 doi:10.1242/jcs.179663

cells, the mechanism of cell migration is independent of PI3K activation.

We next aimed to determine the speed of migration in N1shSHIP2 cells after introducing either GFP–SHIP2 (wild type) or the GFP–SHIP2 (D607A) catalytic mutant. As shown by live-cell imaging, cell velocity was decreased in cells expressing GFP–SHIP2 (wild-type) by 74% as compared to cells with GFP alone. Cells transfected with GFP–SHIP2 D607A had a small yet significant reduction in migration; cell velocity was reduced by 20% (Fig. S2C; Movie 2). Therefore, SHIP2 negatively controls cell migration in N1 cells by a mechanism that is not dependent on PI3K but appears to depend on phosphoinositide phosphatase activity. We verified that pAkt S473 was very much decreased in the presence of the PI3K inhibitors used at the same concentrations (Fig. S1B).

Cell migration was decreased in SHIP2 depleted LN229 glioblastoma cells

We addressed the question of whether our observations in N1 cells could be generalized to other glioblastoma cell lines. For this, we chose the PTEN-containing cell line LN229 and the same lentiviral constructs previously used to infect N1 cells to generate LN229shSHIP2(1) and LN229shSHIP2(2) cells. Western blot analysis shows that SHIP2 expression was reduced by ∼60% in the two SHIP2-depleted cells as compared to LN229 with scramble shRNA Fig. 3A. Cell migration was significantly reduced in the SHIP2-depleted cells (Fig. 3B,C). Interestingly, LY-294002 inhibited cell velocity both in the LN229 control and SHIP2-depleted cells (Fig. 3C). Therefore, the SHIP2-mediated negative control of cell migration in N1 cells cannot be generalized to other glioblastoma cell lines (i.e. LN229 cells).

SHIP2 staining at the plasma membrane partially overlaps with PI(4,5)P2 immunoreactivity in glioblastoma

In order to explain our observations in N1 cells, we first characterized the intracellular localization of SHIP2 in relation to its substrates. Data reported by Hammond et al. have established conditions that allow PI(4,5)P2 immunostaining at the plasma membrane (Hammond et al., 2009). These conditions involve the absence of ‘Triton X-100’ to permeabilize the cells and the use of ‘saponin’ (as outlined in the Materials and Methods section) to stain PI(4,5)P2. We thus addressed the question of the intracellular localization of SHIP2 using the conditions described in Hammond et al. Fixed N1 cells were stained for PI(4,5)P2, PI(3,4,5)P3 and total SHIP2 (Fig. 4A). We found that a large proportion of the total SHIP2 was at the plasma membrane and partly colocalized with PI(4,5)P2. This result very much depended on the immunostaining being performed in the absence of Triton X-100 (data not shown). This result could be generalized to two distinct glioblastoma cell lines (U-87 MG and LN229) and, importantly, to three primary cultures of human glioblastoma (Fig. 4B; Fig. S3A). The same result was observed despite variable amounts of SHIP2 being present at the plasma membrane in different primary cultures. Western blot analysis confirmed the expression of SHIP2, pSHIP2 S132 and PTEN in primary cells (two primary cell cultures of glioblastoma are shown in Fig. S3B). We conclude that in glioblastoma cell lines and primary cultures, SHIP2 can be localized at the plasma membrane where, at least partially, it overlaps with PI(4,5)P2.

SHIP2 controls both PI(4,5)P2 and PI4P at the plasma membrane of N1 cells

As PI3K inhibitors failed to inhibit migration of N1 cells, we hypothesized that PI(4,5)P2 might be the relevant SHIP2 substrate to explain our data. SHIP2 depletion would change the relative content of PI(4,5)P2 and PI4P at the plasma membrane provided PI(4,5)P2 is a genuine cellular SHIP2 substrate. A representative staining of PI(4,5)P2 in N1 vector control and N1shSHIP2 is shown in Fig. 4C. In the same cells, SHIP2 immunoreactivity in N1shSHIP2 cells is reduced by 90% compared to its control value

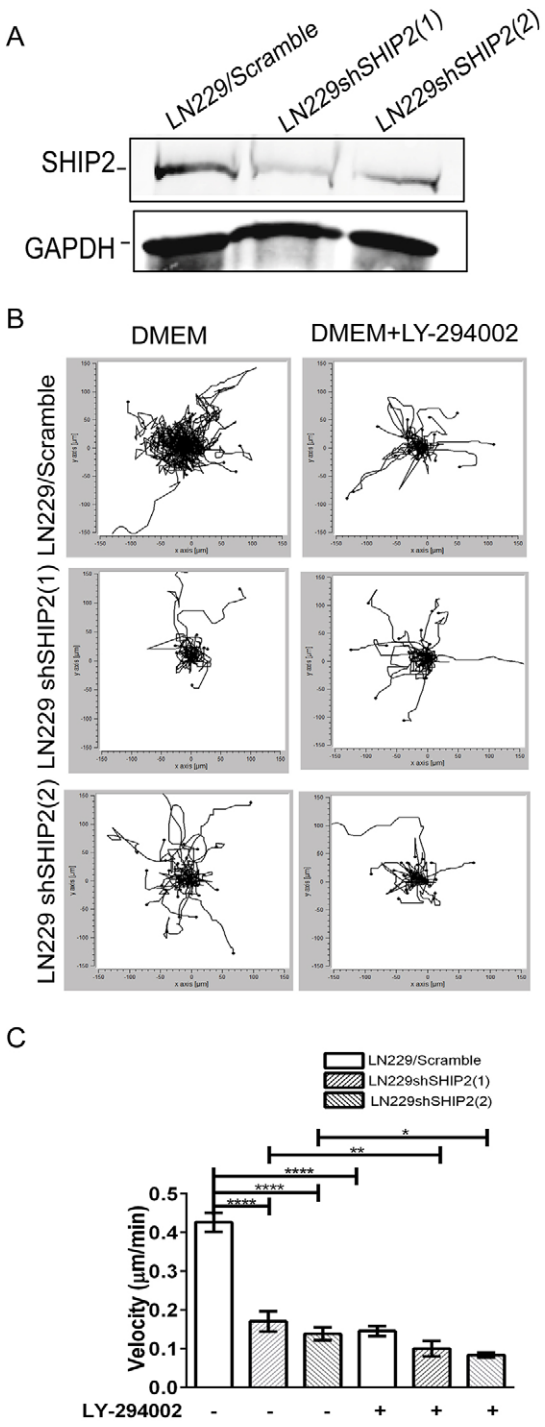

Fig. 3. Migration of SHIP2-depleted LN229 cells. (A) Western blot analysis of SHIP2 and GAPDH in total cell lysates of LN229 cells expressing scrambled shRNA (LN229/Scramble) or one of two SHIP shRNAs [LN229shSHIP2(1) or LN229shSHIP2(2)] maintained in 10% serum. (B,C) Migration was followed and analyzed as described in Fig. 2B,C, *P<0.05; **P<0.005; ****P<0.0001 (Student’s t-test for unpaired data followed by a Mann–Whitney test).

Journal of Cell Science (2016) 129, 1101-1114 doi:10.1242/jcs.179663

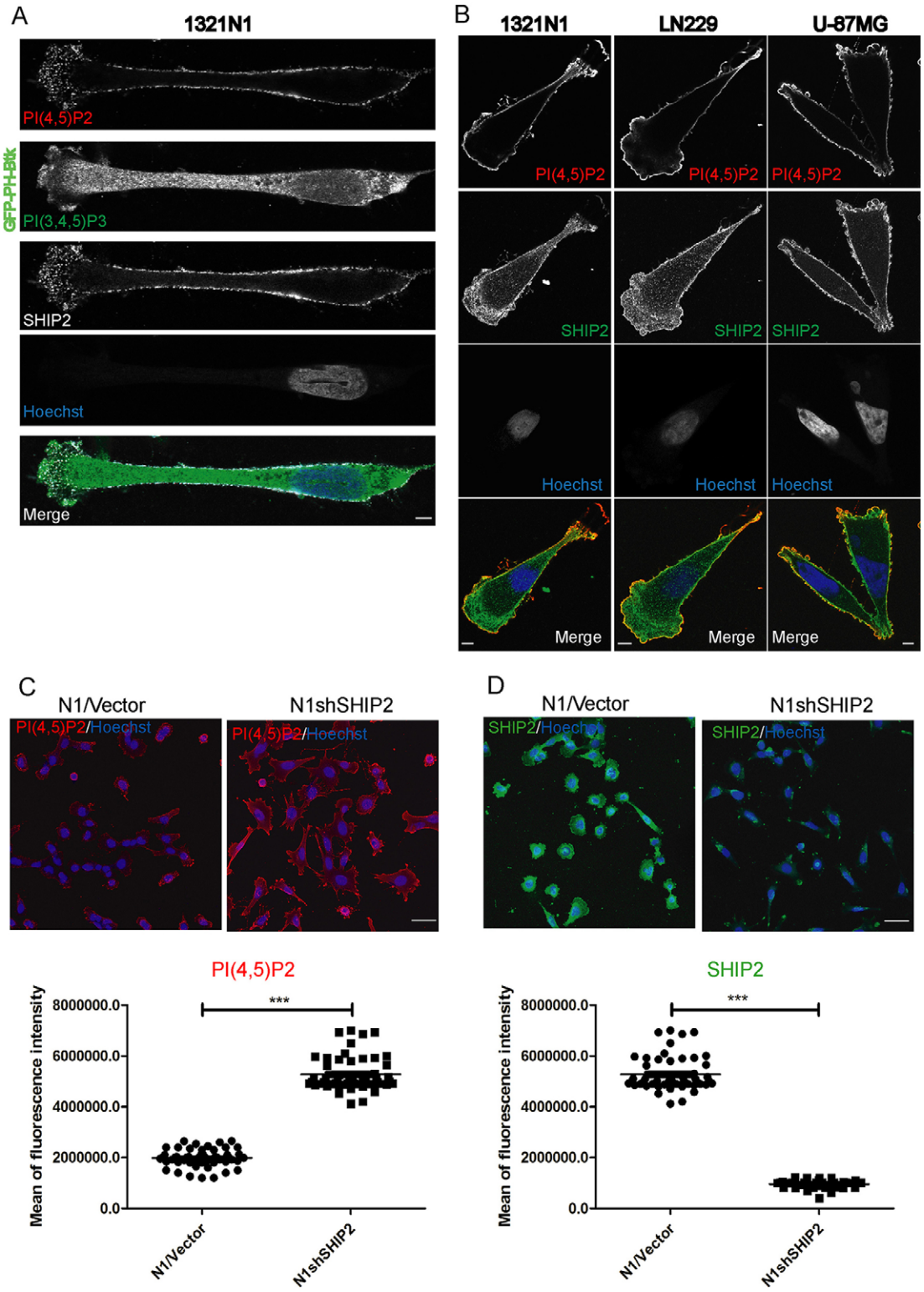

Fig. 4. SHIP2 and PI(4,5)P2 localization at the plasma membrane in glioblastoma cell lines. (A) Immunostaining of PI(4,5)P2, PI(3,4,5)P3 and SHIP2 in N1 cells. GFP–PH-Btk-transfected N1 cells plated on coverslips were fixed and stained with anti-PI(4,5)P2, anti-SHIP2 and anti-GFP antibodies. (B) Immunostaining of endogenous PI(4,5)P2 and SHIP2 in human glioblastoma cell lines. Nuclei were stained with Hoechst 33342 in blue. Images were obtained by confocal microscopy. (C) Immunostaining of endogenous PI(4,5)P2 in N1 vector control (N1/Vector) and N1shSHIP2 cells. The PI(4,5)P2 plasma membrane signal was quantified at 20× as the mean of the fluorescence intensity. Each point represents a measurement of a single field of cells. Bars represent mean fluorescence of several fields. ***P<0.0001 (Student's t-test for unpaired data followed by a Mann–Whitney test). (D) Immunostaining of endogenous SHIP2 in N1/Vector and N1shSHIP2 cells. Cells were visualized using Zeiss LSM780 with a 20× objective (NA 0.8). Nuclei were stained with Hoechst 33342 in blue. The SHIP2 signal was quantified as the mean of fluorescence intensity. Data are mean±s.e.m. (2000 cells). The SHIP2 signal was quantified as the mean of the fluorescence intensity as in C. Bars represent mean fluorescence intensity of several fields (in total of 2000 cells). ***P<0.0001 (Student's t-test followed by Mann–Whitney test). Scale bars: 5 µm (A,B); 50 µm (C,D).

Journal of Cell Science (2016) 129, 1101-1114 doi:10.1242/jcs.179663

(Fig. 4D). PI(4,5)P2 was indeed increased by twofold in N1shSHIP2 cells compared to control or vector-transfected cells (Fig. 4C). In contrast, membranous PI4P was decreased by 60% in SHIP2-deficient cells as compared to SHIP2-containing N1 vector control cells (Fig. 5A). Transfection experiments where we reintroduced X-press-tagged wild-type or phosphatase-dead SHIP2 in N1shSHIP2 cells showed that PI(4,5)P2 was decreased in wild-type SHIP2-transfected cells as compared to in cells with phosphatase-dead SHIP2 D607A (Fig. 5B). This was inverted when PI4P was quantified: PI4P was increased in wild-type SHIP2-transfected cells as compared to the mutated SHIP2 (Fig. 5C). Thus, the observed changes in the PI(4,5)P2-to-PI4P ratio at the plasma membrane in SHIP2-depleted N1 cells are dependent on depletion of SHIP2 catalytic activity.

The use of protein domains for the detection of phosphoinositides as biosensors has been reported in previous studies (Davies et al., 2014; Ooms et al., 2015). Fluorescence intensity has been determined in N1 vector control cells or N1shSHIP2 cells transfected with GFP–PH-PLCδ1, used as a probe for PI(4,5)P2 (Stauffer et al., 1998). We have taken into account all cells that were positive for GFP (i.e. transfected by the probe). We observed a 2.3-fold increase in fluorescence intensity in N1shSHIP2 as compared to N1 vector control cells (Fig. 6A) in agreement with the PI(4,5)P2 antibody data. We also used GFP–PH-TAPP1 to monitor the content of PI(3,4)P2. The staining of this biosensor was abundant in lamellipodia but decreased in N1shSHIP2 cells compared to control (Fig. 5D).

Given that our data suggested an important role of PI(4,5)P2 is the control of cell migration in N1shSHIP2 cells, we asked whether migration would be affected when blocking PI(3,4,5)P3 or PI(4,5)P2 by overexpression of a specific probe for each lipid. We therefore transfected GFP–PH-Btk [a biosensor of PI(3,4,5)P3] and GFP–PH-PLCδ1 in N1 shSHIP2 cells. Live cell imaging shows that GFP–PH-Btk decreases cell migration by reducing cell velocity by 17% whereas GFP–PH-PLCδ1 reduces velocity by 65% (Fig. 6B; Movie 3). The data suggest that PI(4,5)P2 plays a major role in the control of cell migration. We also determined *in vivo* protrusion dynamics in N1 vector control and N1shSHIP2 cells by bright-field dynamics: SHIP2-depleted cells showed significantly more protrusions as compared to N1 vector control cells (Fig. S3C,D). Finally, we estimated the levels of PI(4,5)P2 and PI4P after labeling the cells with ^{32}P. The ratio of PI(4,5)P2 to PI4P was significantly increased in N1shSHIP2 cells as compared to N1 vector control (Fig. S3E).

We conclude that in N1 cells, SHIP2 controls the balance between PI(4,5)P2 and PI4P at the plasma membrane consistent with its previously established catalytic activity towards PI(4,5)P2 *in vitro* (Giuriato et al., 2002; Nakatsu et al., 2010; Taylor et al., 2000; Vandeput et al., 2007). In addition, it is involved in controlling the PI(3,4,5)P3–PI(3,4)P2 balance in lamellipodia.

Quantification of pFAK Y397, paxillin and vinculin staining in N1 deficient cells

PI(4,5)P2 has several downstream cellular effectors. It activates focal adhesion kinase (FAK, also known as PTK2) by a combination of clustering and conformational changes that promote efficient autophosphorylation (Goni et al., 2014). Consistent with SHIP2-mediated control of PI(4,5)P2 levels, western blotting showed that FAK phosphorylated at Y397 (pFAK Y397) was upregulated in N1shSHIP2 cells as compared to control cells, with no change in the total levels of FAK (Fig. 7A). Focal adhesion length was quantified by determining the length of pFAK Y397 staining in N1 control and N1 SHIP2-deficient cells (Fig. 7B). This was based on the report that the mean length of focal adhesions precisely predicts cell speed and migration (Kim and Wirtz, 2013). The quantification was made in the absence and presence of fetal calf serum (FCS) for 30, 60 and 120 min. The focal adhesion length was increased in N1shSHIP2 cells as compared to control cells at any time of FCS stimulation and even in the absence of any stimulation (Fig. 7B, right panel). Similar results were obtained using two other focal adhesion proteins, paxillin and vinculin (Fig. 7C,D), with a clear impact on F-actin staining (Fig. 7E). We conclude that, besides upregulation of pFAK Y397, focal adhesion length is specifically increased in SHIP2-deficient cells, suggestive for focal adhesion turnover controlled by SHIP2.

SHIP2 interaction with myosin-1c and filamin A in N1 cells

SHIP2-interacting proteins are often cytoskeletal and focal adhesion proteins (reviewed in Elong Edimo et al., 2013). SHIP2 is part of the integrin adhesome network (Wolfenson et al., 2013) and localizes to circular dorsal ruffles (Hasegawa et al., 2011), which are important structures implicated in the initiation of cell migration. We asked whether SHIP2 localization in N1 cells also involves focal adhesion proteins and/or PI(4,5)P2-binding proteins. Potential SHIP2-binding proteins co-immunoprecipitating with SHIP2 were subjected to mass spectrometry analysis. Preimmune serum was used as a negative control (Fig. S4A). A staining of SHIP2 immunoprecipitated proteins allowed the identification of known SHIP2 interactors based on published data in other cell types [e.g. Dok1 and intersectin (Cunningham et al., 2010; Nakatsu et al., 2010; Xie et al., 2008)]. In addition, the actin-binding and PI(4,5)P2-binding protein myosin-1c (Myo1c) was identified as a new potential interactor with a Mascot score of 857. The interaction between SHIP2 and Myo1c was confirmed by co-immunoprecipitation in N1 cells at endogenous level (Fig. S4B,C). The previously identified SHIP2 interactor and actin-binding protein filamin A [in COS-7 cells (Dyson et al., 2001)] was also present in the SHIP2 immunoprecipitate (Fig. S4C). Conversely, SHIP2 and Myo1c were present when filamin A was immunoprecipitated and the blot probed with anti-SHIP2 and anti-Myo1c antibodies (Fig. S4D).

DISCUSSION

In this study, we provide evidence of a negative control of SHIP2 in cell migration in PTEN-null glioblastoma 1321 N1 cells. This was shown in cells depleted of SHIP2 by the use of three different shRNAs. The migration defect could be rescued in N1shSHIP2 cells by introducing GFP–SHIP2 but not its catalytic mutant. Therefore, the mechanism controlling migration involves SHIP2 phosphatase activity, which modulates of the balance between PI(4,5)P2 and PI4P and changes in focal adhesion dynamics. In N1 cells, cell migration was not inhibited by the two PI3K inhibitors we have tested. However, PI3K inhibitors do inhibit cell migration in a different glioblastoma cell line LN229 cells. In LN229 cells, depletion of SHIP2 inhibited cell migration. Hence, the negative control of SHIP2 on cell migration in N1 cells is dependent on the cell type and varies between different glioblastoma cells.

We show for the first time SHIP2 immunostaining at the plasma membrane in very distinct glioblastoma cell lines and human primary cultures. SHIP2 immunoreactivity partly overlaps with the staining of PI(4,5)P2. Overall these findings were unexpected as SHIP2 was essentially reported to be perinuclear and to translocate at the plasma membrane in the presence of growth factors or insulin (Ishihara et al., 2002; Onnockx et al., 2008; Pesesse et al., 2001; Takabayashi et al., 2010; Wang et al., 2004). We have shown in this

Journal of Cell Science (2016) 129, 1101-1114 doi:10.1242/jcs.179663

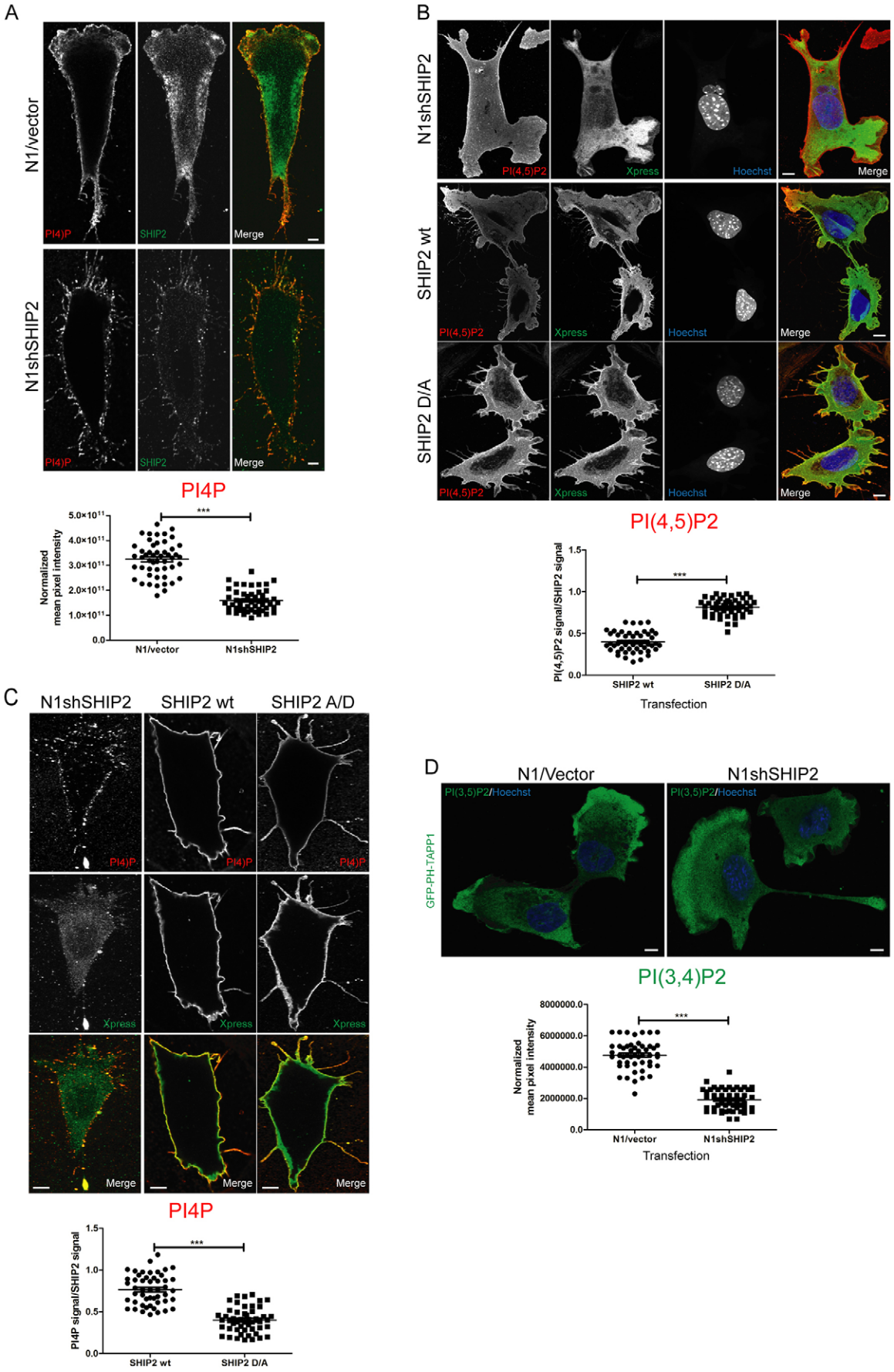

Fig. 5. See next page for legend.

Journal of Cell Science

Journal of Cell Science (2016) 129, 1101-1114 doi:10.1242/jcs.179663

Fig. 5. SHIP2 transfection in N1shSHIP2 cells affects plasma membrane PI(4,5)P2 and PI4P levels. (A) Immunostaining of PI4P in N1 vector control (N1/Vector) and N1shSHIP2 cells. After 5 min of stimulation with 10% FCS, cells were fixed and stained for PI4P and SHIP2. The PI4P plasma membrane signal was quantified. Each point represents a measurement of a single cell; bars represent normalized mean fluorescence (50 cells). ***P<0.0001 (Student's t-test followed by Mann–Whitney test). (B) N1shSHIP2 cells transfected with X-press-tagged wild-type SHIP2 (wt) or X-press-tagged SHIP2 D607A (D/A, catalytic mutant) cells were plated on coverslips and cultured in the presence of 10% FCS for 24 h before starvation. After 5 min of stimulation with 10% FCS, cells were fixed and stained with PI(4,5)P2 and Xpress. The PI(4,5)P2 plasma membrane signal was quantified. Each point represents a measurement of the PI(4,5)P2 to Xpress ratio from a single cell. Bars represent normalized mean fluorescence. ***P<0.0001 (Student's t-test followed by Mann–Whitney test). (C) N1shSHIP2 cells transfected with X-press-tagged wild-type SHIP2 or X-press-tagged SHIP2 D607A (catalytic mutant) cells were plated on coverslips and cultured in the presence of 10% FCS for 24 h before starvation. After 5 min of stimulation with 10% FCS, cells were fixed and stained with PI4P and Xpress. The PI4P plasma membrane signal was quantified. Each point represents a measurement of the PI4P to Xpress ratio from a single cell. Bars represent normalized mean fluorescence. ***P<0.0001 (Student's t-test followed by Mann–Whitney test). (D) N1shSHIP2 cells transfected with GFP–PH-TAPP1 to probe PI(3,4)P2 were plated on coverslips and cultured in the presence of 10% FCS for 24 h before starvation. After 5 min of stimulation with 10% FCS, cells were fixed and stained for GFP. The PI(3,4)P2 signal was quantified. Each point represents a measurement of PI(3,4)P2 after normalization from a single cell. Bars represent normalized mean fluorescence. ***P<0.0001 (Student's t-test followed by Mann–Whitney test). In B–D, nuclei were stained with Hoechst 33342 in blue, and cells were visualized using Zeiss LSM780 and a 63× oil objective (NA 1.46). Scale bars: 5 µm.

study that the conditions that preserve plasma membrane staining for PI(4,5)P2 (Hammond et al., 2009) also apply to staining of SHIP2. It will be interesting to use the same conditions to stain and compare other members of the phosphoinositide 5-phosphatase family.

SHIP2 immunoreactivity partially overlaps with PI(4,5)P2 immunoreactivity in N1 cells and other glioblastoma cell lines and primary cultures, arguing that the lipid phosphatase might perhaps control PI(4,5)P2 in several glioblastoma cell types. We have reported that PI(4,5)P2 in the nucleus was elevated in N1shSHIP2 cells as compared to control cells (Elong Edimo et al., 2011). We have now quantified PI(4,5)P2 at the plasma membrane of the same cells both by the use of antibodies and a PI(4,5)P2 biosensor (Stauffer et al., 1998). The conclusion is similar for both techniques: PI(4,5)P2 at the plasma membrane is elevated in N1shSHIP2 cells compared to control. To further support a role of PI(4,5)P2, we overexpressed a specific probe for either PI(3,4,5)P3 or PI(4,5)P2 to see whether migration was affected in N1shSHIP2 cells. We observe a minor decrease in migration in cells expressing GFP–PH-Btk, a biosensor for PI(3,4,5)P3 but in contrast a major effect on migration in cells expressing GFP–PH-PLCδ1, a biosensor for PI(4,5)P2 in N1shSHIP2 cells. PI(4,5)P2 therefore plays a major role in the control of cell migration in this cell line. Finally, data reported by the group of Anderson shows that type I γ phosphatidylinositol 4-phosphate 5-kinase (PIPKIγ) knockdown cells have fewer protrusions as compared to control cells (Choi et al., 2013) and that serum-induced migration was significantly attenuated by PIPKIγ knockdown. This indicates that migration and lamellipodium formation require PIPKIγ and PI(4,5)P2 (Choi et al., 2013). We quantified the protrusions by live-cell imaging in SHIP2-depleted N1 cells as compared to N1 vector control cells, and we see more protrusions in N1shSHIP2 as compared to N1 vector control cells. This result is consistent with an increase in PI(4,5)P2 in N1shSHIP2 cells compared to control.

Previous data from the De Camilli laboratory has shown that in COS-7 cells, SHIP2 was concentrated at endocytic clathrin-coated pits during early stages of their maturation (Nakatsu et al., 2010). The possibility was presented that SHIP2 might cause PI(4,5)P2 to decline. It, however, remained unclear whether altered clathrin-coated pit dynamics is a consequence of change in the levels of PI(3,4,5)P3, PI(4,5)P2 or both (Posor et al., 2015). Based on our data, we suggest that SHIP2 metabolizes both substrates PI(3,4,5)P3 and PI(4,5)P2: in our model of glioblastoma (N1 cells), PI(3,4,5)P3 modulation has an impact on cell proliferation, whereas PI(4,5)P2 modulation is a key factor in the control of cell migration. Interestingly, PIPKIγ, which produces PI(4,5)P2, targets and regulates focal adhesions (Ling et al., 2002). The PI(4,5)P2-generating enzyme interacts with the cytoskeletal regulator IQGAP1 and functions together in the regulation of directional cell migration (Choi et al., 2013). Overall, it thus appears that PI(4,5)P2 levels can be controlled by multiple mechanisms both for its production and for its dephosphorylation by SHIP2.

SHIP2 is part of the adhesome and can interact with a large number of cytoskeletal and focal adhesion proteins, and particularly with filamin A (Dyson et al., 2001), vinexin (Paternotte et al., 2005), intersectin (Nakatsu et al., 2010; Xie et al., 2008), RhoA (Kato et al., 2012) and, as shown here in N1 cells, Myo1c. Using the same SHIP2 immunoprecipitation and washing conditions used in N1 cells, we could not show the presence of Myo1c in SHIP2 immunoprecipitates from COS-7 lysates (data not shown). This suggests that the presence of the SHIP2–Myo1c complex might be rather specific for N1 cells. Interestingly, in a different cell type, nephrin regulates lamellipodia formation by assembling a protein complex that includes SHIP2, filamin and lamellipodin (Venkatareddy et al., 2011). SHIP2 is part of the adhesome, and it has been proposed that, on average, each adhesome protein has approximately nine different potential partners (Zaidel-Bar and Geiger, 2010). This is in agreement with our data and suggests that a complex of cytoskeletal proteins, as identified in N1 cells, is constantly interacting with SHIP2. We have shown that N1shSHIP2 cells transfected with a SHIP2 catalytic mutant, GFP–SHIP2 D607A, had a small yet significant reduction in migration (i.e. 20%) as compared to cells transfected with GFP alone. This suggests that docking properties of SHIP2 might also influence cell migration. We speculate that this contributes to the specificity of SHIP2 acting through both its phosphatase activity and intrinsic docking properties (Erneux et al., 2011).

Reports in the literature reveal that the function of SHIP2 as a pro- or anti-oncogene is not clear and very much depends on the cellular model (Elong Edimo et al., 2011; Prasad et al., 2008a; Taylor et al., 2000). In breast cancer cells, where it has been mostly studied, SHIP2 participates in the mechanism of invadopodium maturation by producing the key lipid PI(3,4)P2 (Sharma et al., 2013). As PI(3,4,5)P3 is considered as the major SHIP2 substrate (Balla, 2013; Vandeput et al., 2007), the PI3K–Akt pathway is often upregulated in SHIP2-depleted cells as compared to control cells. This was the case in SHIP2-depleted N1 cells compared to control cells (Elong Edimo et al., 2011). Therefore, SHIP2 can be considered as a tumor suppressor in some cells; for example, in keratinocytes (Yu et al., 2008) and in PTEN-deficient glioblastoma (Elong Edimo et al., 2011; Taylor et al., 2000). Cell migration is a fundamental mechanism in physiology but also in many diseases such as cancer (Sun et al., 2013). Here, as well, as also reported in other studies, the influence of SHIP2 on cell migration varies from one cell type to the other. For example, silencing SHIP2 in HEK293 cells increases cell migration, but in U251 glioma cells depletion of SHIP2 attenuates cell polarization and migration (Kato

Journal of Cell Science (2016) 129, 1101-1114 doi:10.1242/jcs.179663

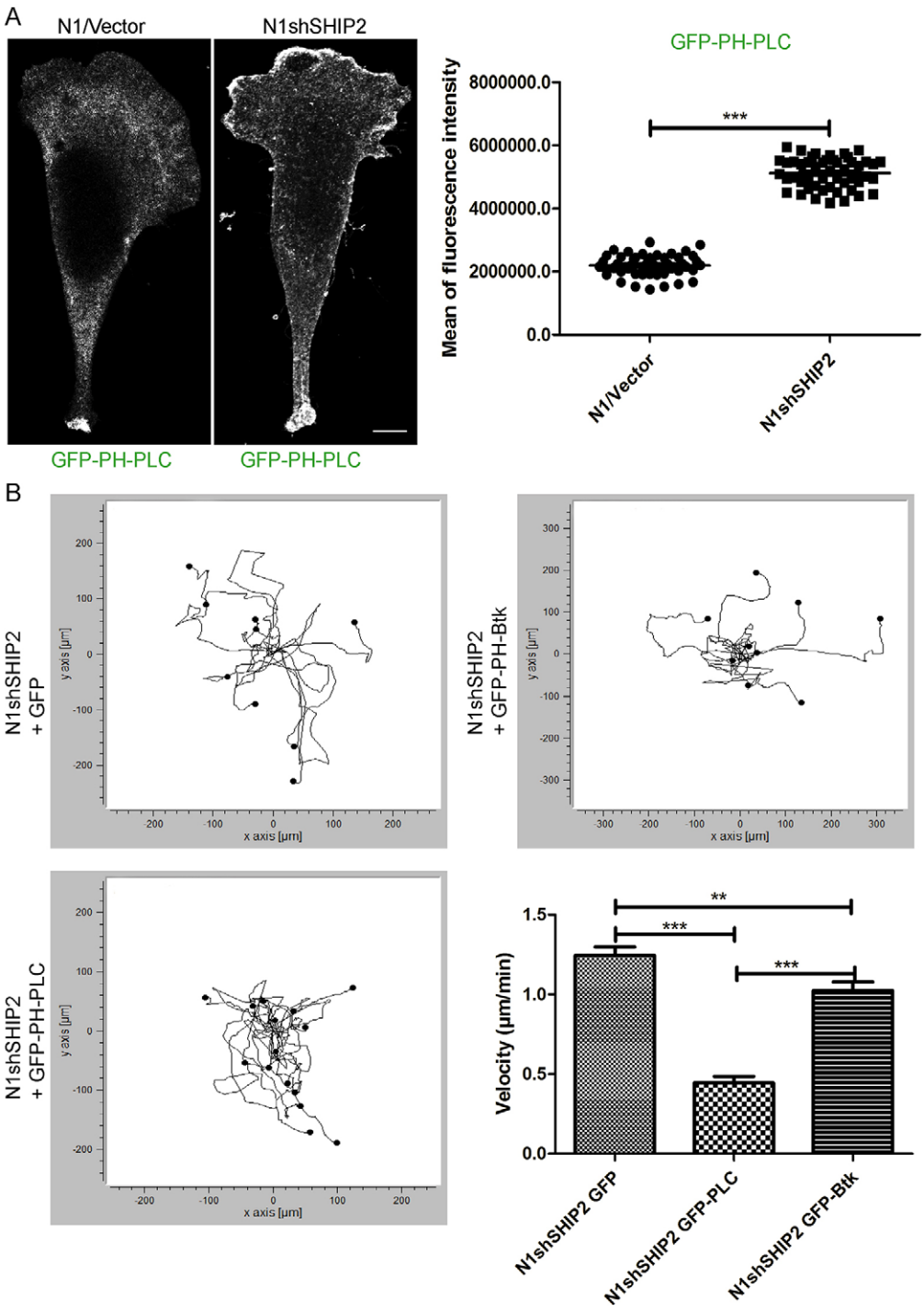

Fig. 6. Inhibition of cell migration visualized using the biosensor GFP–PH-PLCδ in N1shSHIP2 cells. (A) N1 vector control (N1/Vector) and N1shSHIP2 cell lines were plated on 3-cm tissue culture dish and transfected with GFP–PH-PLCδ for 24 h. Cells were plated on coverslips. Representative images of GFP immunostaining are shown. Scale bar: 50 µm. Each point represents a measurement of a single cell; bars represent mean fluorescence. GFP–PH-PLCδ fluorescence intensities. 100 cells for each cell line were analyzed and scored for three independent transfections. ***P<0.0001 compared with vector control cells (Student's t-test for unpaired data followed by Mann–Whitney test). (B) Individual cell migration of N1shSHIP2 cells transfected with GFP, GFP–PH-PLCδ and GFP–PH-Btk tracked over time and depicted as the ratio of axial (y-axis) to tangential (x-axis) motility. The data depicts a minimum of eight representative cells in three independent experiments. Cell velocity is graphically depicted as mean±s.e.m. ***P<0.0001 compared with control (Student's t-test for unpaired data as in Fig. 2).

et al., 2012; Yu et al., 2010). Kato et al. interpreted their data by showing an association between SHIP2 and RhoA and observed an impairment of proper PI(3,4,5)P3 localization in SHIP2-depleted U251 cells (Kato et al., 2012). In this model, PI(3,4,5)P3 at the leading edge was very much decreased both in SHIP2-depleted cells as compared to control cells and in the presence of the PI3K inhibitor LY-294002. The levels of PI(4,5)P2 at the plasma membrane were not reported in this study. We suggest an alternative explanation based on the ability of SHIP2 to recognize PI(4,5)P2 as substrate, in addition to PI(3,4,5)P3 (Fig. 8). It will be interesting to establish whether this last mechanism can apply in U251 cells.

The importance of PI(3,4)P2 interaction with lamellipodin and its function in migration and endocytosis has been reported (Krause and Gautreau, 2014). In our model of N1 cells, we have seen that PI(3,4)P2 is actually decreased in SHIP2-depleted N1shSHIP2 cells as compared to N1 vector control cells. Neither PI3K inhibitors nor Akt inhibitors (Akti; W.E.E., unpublished data) influence cell migration in N1 vector control or N1shSHIP2 cells. This suggests that migration is not controlled by a PI(3,4,5)P3–PI(3,4)P2 pathway in our model cell line (Fig. 8). Other phosphoinositides, in particular PI(4,5)P2, have been reported to modulate cytoskeletal organization and cell migration (Choi et al., 2015; Sun et al., 2013; Tsujita and Itoh, 2015). PI(4,5)P2 binding of IQGAP1 is important for cell morphology and migration,

Journal of Cell Science (2016) 129, 1101-1114 doi:10.1242/jcs.179663

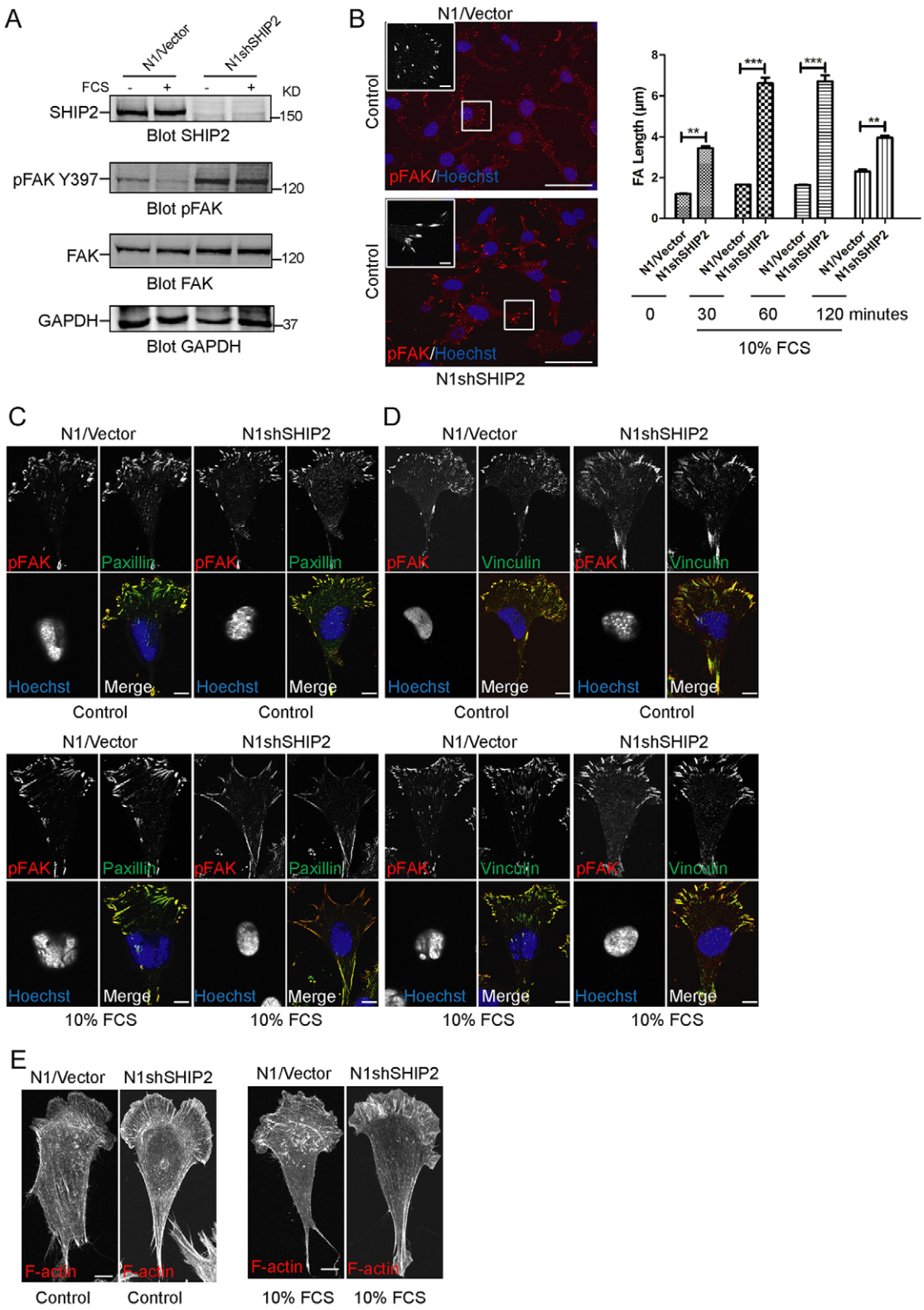

Fig. 7. SHIP2 controls focal adhesion dynamics in N1 cells. (A) SHIP2, pFAK Y397, and total FAK expression were determined in cell lysates from N1 vector control (N1/Vector) and N1shSHIP2 cells unstimulated or stimulated with 10% FCS. (B) SHIP2 controls the focal adhesion dynamics. N1/Vector and N1shSHIP2 were serum starved (left panel) and stained for pFAK Y397. Nuclei were stained with Hoechst 33342 in blue. Cells were visualized using a Zeiss LSM780 63× oil objective (NA 1.46). Scale bars: 50 µm (main image), 5 µm (inset). The right panel shows a quantification of the focal adhesion length of starved cells and stimulated with 10% FCS for 30, 60 and 120 min at 37°C. Focal adhesion length was measured in 60 cells in three independent experiments and expressed as the mean±s.e.m. ***P*<0.01; ****P*<0.001 (two-way ANOVA followed by Bonferroni post-test). (C) Immunocytochemistry of pFAK Y397 and Paxillin in N1/vector and N1shSHIP2 cells. (D) Immunocytochemistry of pFAK Y397 and Vinculin in N1/vector and N1shSHIP2 cells. (E) Immunostaining of F-actin in N1/vector and N1shSHIP2 cells. In C–E, cells were unstimulated or stimulated with 10% of FCS for 5 min. Nuclei were stained with Hoechst 33342 in blue, and cells were visualized using a Zeiss LSM780, 63× oil objective (NA 1.46). Scale bars: 5 µm.

Journal of Cell Science (2016) 129, 1101-1114 doi:10.1242/jcs.179663

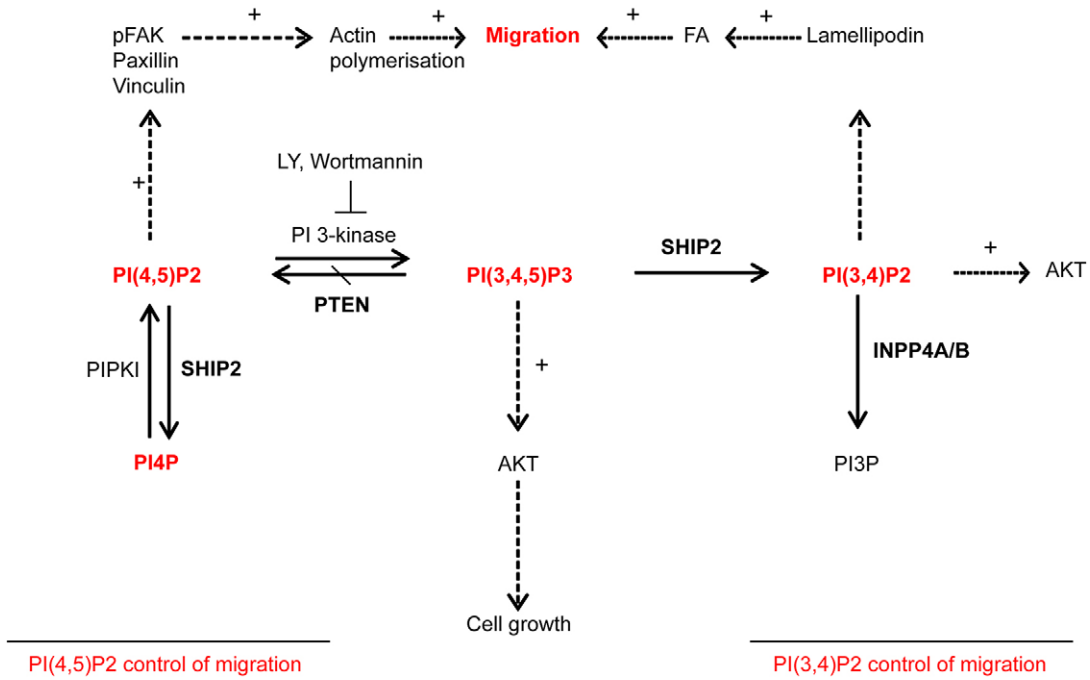

Fig. 8. A model depicting two control mechanisms by which phosphoinositides modulate cell migration. In PTEN-null 1321 N1 cells, SHIP2 could act on two substrates PI(3,4,5)P3 and PI(4,5)P2. Migration was not affected in the presence of PI3K inhibitors. PI(4,5)P2 is upregulated in SHIP2-depleted cells, thereby controlling focal adhesion (FA) dynamics and cell migration.

and lamellipodium formation also requires PIPKIγ (Choi et al., 2013). Our data suggest that, in N1 cells, SHIP2 controls PI(4,5)P2 levels, which could control focal adhesions and/or possibly IQGAP1 activity. PI(4,5)P2 is an upstream activator of pFAK Y397 in focal adhesions and has been reported to change cell attachment and spreading (Goni et al., 2014). We observed that pFAK Y397 is actually upregulated in SHIP2-deficient cells as compared to control cells. This has a positive impact on focal adhesion length (pFAK Y397 immunoreactivity) and cell migration (Fig. 8).

We have evidence that in PTEN-positive LN229 cells, migration is decreased in SHIP2-depleted cells. The reason for this is not yet understood; we speculate that the content of the different phosphoinositides PI(4,5)P2, PI(3,4)P2 and PI(3,4,5)P3 could be very different between cell types. Our data in primary glioblastoma show that PI(4,5)P2 levels, as assessed by immunostaining, are very different between different primary cell cultures. In support of this, SHIP2 and PTEN levels determined by western blotting are quite different in different primary human glioblastoma cells from different patients (W.E.E., unpublished data). SHIP2 could be highly expressed, expressed at low levels or even absent, and the same applies for PTEN. In glioblastoma, intratumor heterogeneity of PTEN expression is well known and reflects cancer evolutionary dynamics (Sottoriva et al., 2013). It is likely that the same concept would apply for SHIP2 and other members of the inositol polyphosphate 5-phosphatase family [e.g. INPP5K (Davies et al., 2014)]. It would be interesting to establish whether loss of PTEN correlates with a role for SHIP2 in migration in different primary cultures of human glioblastoma with different genotypes.

MATERIALS AND METHODS

Reagents

Anti-SHIP2 monoclonal antibody used for total SHIP2 immunostaining was from Novus (Cambridge, UK; catalog number H00003636-M01). It was initially characterized in Deneubourg et al., 2014; McNulty et al., 2011 and used at 1:300. Anti-SHIP2 antibodies used in immunoprecipitation have been characterized previously (Muraille et al., 1999). Anti-SHIP2 antibody phosphorylated on S132 was custom-made in the laboratory (Elong Edimo et al., 2011). The monoclonal antibody against the filamin A N-terminal (5–40 amino acids) (catalog number sc-17749) was from Santa Cruz Biotechnology (Heidelberg, Germany) and was used at 1:500 dilution. Myo1c polyclonal antibody (catalog number M3567, used at 1:1000), vinculin antibody (catalog number V4505, used at 1:300), Erk inhibitor U0-126 (catalog number U120), LY294002 hydrochloride (catalog number L9908) and wortmannin (catalog number W-1628) were from Sigma-Aldrich (Diegem, Belgium). Polyclonal pFAK Y397 and total FAK antibodies (catalog number 3283 and 3285) were from Cell Signaling Technology (Bioke, The Netherlands; used at 1:350 and 1:100, respectively). Antibodies against pAkt S473 (catalog number, 9271 L), pAkt T308 (catalog number, 9275L) and total Akt (catalog number, 9272S) were from Cell Signaling Technology and used at 1:500. Paxillin antibody 5H11 (catalog number 3127) was from Abcam (Cambridge, UK used at 1:300). Antibodies to PI(4,5)P2 (2C11) (catalog number sc-53412, used at 1:200) and PI4P (catalog number s-P004, used at 1:50) were from Santa Cruz Biotechnology and Echelon (Le-Perray-en-Yvelines, France), respectively. Myo1c shRNA plasmid (h) (catalog number sc-44604-SH) was from Santa Cruz Biotechnology. Protein A Sepharose™ CL-4B was from GE Healthcare Bio-Sciences (Diegem, Belgium). Lipofectamine™ (catalog number 11668-019), Alexa-Fluor-594-conjugated phalloidin (catalog number A12381), Alexa-Fluor-488-conjugated donkey (catalog number A21206) and Alexa-Fluor-594-conjugated goat (catalog number A11012) anti-rabbit-IgG, Alexa-Fluor-488-conjugated donkey (catalog number A21202) and Alexa-Fluor-594-conjugated goat (catalog number A11032) anti-mouse-IgG, Hoechst 33342 (catalog number H-3570) and normal goat serum (reference 16210-064) were from Invitrogen (Breda, The Netherlands). The Glycergel mounting medium (catalog number C0563) was from Dako (Heverlee, Belgium). mRFP or GFP-tagged PH-PLCδ1, GFP–PH-Btk, GFP–PH-TAPP1 were provided by Tamas Balla (NIH, USA). The X-press-tagged SHIP2 wild-type and catalytic mutants are as reported previously (Pesesse et al., 2001). GFP–SHIP2 was kindly provided by Chris Mitchell (Monash University, Australia). The GFP–SHIP2 catalytic mutant (D607A) was supplied by MRC-PPU reagents at University of Dundee. We

Journal of Cell Science (2016) 129, 1101-1114 doi:10.1242/jcs.179663

verified that both X-press-tagged SHIP2 and GFP–SHIP2 are active in a phosphatase assay using either PI(3,4,5)P2 or PI(4,5)P2 as substrate (Vandeput et al., 2006).

Cell culture

Human glioblastoma cell lines (1321 N1, LN-229 and T-98G cells) and U-87MG cells were cultured in Dulbecco's modified Eagle's medium (DMEM) (GIBCO, CA), supplemented with 5% fetal calf serum (FCS), 2% penicillin-streptomycin and maintained at 37°C, 5% CO_2. Cells were kindly provided by Isabelle Salmon (Hôpital Erasme, Université Libre de Bruxelles) and Peter Downes (University of Dundee, UK), and have been characterized previously (Elong Edimo et al., 2011, 2013). Cells were regularly checked to be free of mycoplasma. Human glioblastoma specimens were obtained within the framework of a study that received approval from the ethical review board of the University Hospital of Utrecht, The Netherlands, according to the principles of the Declaration of Helsinki. Written informed consent was obtained from the patients prior to surgery. Primary cultures of human glioblastoma were prepared as previously reported (Robe et al., 2004) and maintained anonymously in culture facilities at the laboratory of Human Genetics, University of Liège, Belgium.

Generation of stable shRNA-expressing cells

N1 cells were plated at 1×10^5 cells per well in 12-well plates, 1 day before transfection. Cells were transiently transfected with the desired pSUPER constructs using Lipofectamine™ 2000 (Elong Edimo et al., 2011). After recovery, the cells were selected by incubation for 3 days with 6 µg/ml puromycin. Cells resistant to puromycin were counted, diluted and distributed in 96-well plates so that one cell per well was achieved. Clonal populations were then expanded and analyzed for SHIP2 and Myo1c expression. N1shSHIP2 cells devoid of SHIP2 expression (as analyzed by western blotting) were generated by increasing the puromycin concentration up to 3 µg/ml.

Generation of stable SHIP2 depleted N1 and LN229 glioblastoma cells by lentiviral infection

N1 and LN229 cells were transduced with Sigma MISSION lentiviral transduction particles containing a pLK0.1-Puro plasmid encoding either a non-mammalian shRNA (Scramble SHC02) or one of two SHIP2-specific targeting shRNAs [reference number TRCN 0000052810 and TRCN 0000052808 for sh(1) and sh(2), respectively] at a multiplicity of infection of 2.8 in growth medium supplemented with 8 µg/ml of polybrene overnight at 37°C. Transduced cells were selected in growth medium supplemented with 6 µg/ml puromycin for 3 weeks then subsequently maintained in growth medium without puromycin.

Scratch assay for migration and live-cell imaging

Culture-inserts for self-insertion were obtained from Proxylab and used to generate a scratch. N1 vector control or N1shSHIP2 cells were allowed to migrate for 6–8 h. The migration distance was quantified by ImageJ. Individual cells plated on FluoroDish™ (µ-Dish 35 mm, high, glass bottom from Ibidi) were allowed to migrate and analyzed with a Leica DM6000B microscope for live-cell imaging.

Cell transfection of GFP constructs

N1 vector control or shSHIP2 cells were kept in 5% FCS with no antibiotics for 24 h and were transfected at 90% confluence. For 9-cm diameter cell dishes, 60 µl of Lipofectamine™ 2000 and 24 µg DNA were used according to manufacturer's protocol and cells were allowed to express the constructs for 48 h before lysis.

Proteins extract preparation and immunoprecipitation

N1 cells were lysed in buffer A (10 mM Tris-HCl pH 7.5, 150 mM KCl, 12 mM 2-mercaptoethanol, 100 mM NaF, 0.5% NP-40, 0.01 µM sodium vanadate and 2 mM EDTA) and protease inhibitors (Roche). The cells were scraped, and the lysates were cleared by centrifugation at 14,000 ***g***. The lysates were normalized based on total protein content measured using the Bradford assay. Equal amounts of proteins (3×1 mg) were subjected to incubation with protein-A–Sepharose. After preclearing, the cell lysates were incubated in the presence of antibodies or preimmune sera for 2 h at 4°C. After centrifugation (18,000 ***g*** for 1 min), the immune complexes were washed extensively with ice-cold lysis buffer A and three times with ice-cold lysis buffer B (10 mM Tris-HCl pH 7.5, 500 mM NaCl, 150 mM KCl, 12 mM 2-mercaptoethanol, 100 mM NaF, 0.5% NP-40, 0.01 µM sodium vanadate and 2 mM EDTA) containing protease inhibitors.

Western blotting

Samples were loaded on polyacrylamide gels and run for 1.5 h. Proteins were transferred onto nitrocellulose membranes, blocked in Odyssey blocking buffer (LI-COR Biosciences), incubated with primary antibodies overnight at 4°C. After 3 washes in PBS with Odyssey blocking buffer, membranes were incubated with DyLight 680 anti-rabbit- and anti-mouse-IgG or DyLight 800 anti-rabbit- and anti-mouse-IgG (Thermo Fisher Scientific) for 1 h at room temperature, washed three times in PBS with 0.1% Tween 20 (BioRad). Membranes were scanned using a high sensitivity Odyssey Infrared Imaging System (LI-COR Biosciences).

Identification of SHIP2 interactors by mass spectrometry

Immunoprecipitation was performed as described above, and the precipitates were boiled for 5 min in SDS sample buffer and subjected to SDS-PAGE (8% gels). The gel was stained with Coomassie Blue and destained in 30% methanol in HPLC-grade water. The protein bands of interacting proteins were excised and digested *in situ* with trypsin as described previously (Elong Edimo et al., 2011). The resulting peptides were desalted, concentrated with ZipTip C-18 (Millipore, Bedford, MA) and analyzed using a ABI 4800 matrix assisted laser-desorption ionization (MALDI)–time-of-flight (TOF)/TOF analyzer (Applied Biosystems, CA) with α-cyano-4-hydroxycinnamic acid (5 mg/ml in 50% acetontrile) as the matrix. The tandem mass spectrometry (MS/MS) results were submitted to the Mascot 2.2.0 search engine with UniProtKB as the target database.

Lipid extraction and separation after [^{32}P] labeling

2.5×10^6 N1 cells were cultured overnight in DMEM medium supplemented with 5 % FCS (Elong Edimo et al., 2011). Cells were washed twice in medium without serum and incubated for 24 h in this medium. Cells were then washed twice in medium without serum and without phosphate and labeled for 4 h in medium containing [^{32}P] but not phosphate. The phosphoinositides were measured as described previously (Blero et al., 2005).

Immunofluorescence

Immunostaining in the presence of Triton X-100

Cells plated on coverslips were fixed in 4% paraformaldehyde for 20 min at room temperature and incubated in 10 mM Tris-HCl pH 7.4, 0.15 M sodium chloride (TBS) containing 0.1% (v/v) Triton X-100 (TBS-TX), 10% normal horse serum (NHS) (Hormonologie Laboratoire, Marloie, Belgium) and 10% normal goat serum (NGS) (Invitrogen) for 1 h at room temperature. The coverslips were left overnight at 4°C in a humid chamber with the primary antibodies diluted in TBS-TX containing 1% NHS and 1% NGS; they were then rinsed in TBS and then incubated in the dark for 1 h at room temperature in TBS containing the secondary antibodies. Coverslips were then rinsed in TBS and nuclei were stained with Hoechst 33342 dye 5 µM in Tris-HCl 0.05 M (pH 7.4) for 2 min in the dark at room temperature. Primary antibodies raised in different species and secondary antibodies coupled with different fluorochromes, were combined to specifically label one marker in green (Alexa Fluor 488), the other in red (Alexa Fluor 594). After three rinses in TBS, the coverslips were mounted with Glycergel Mounting Medium anti-fade mounting medium.

Immunostaining in the presence of saponin for PI(4,5)P2 and PI4P staining

Cells plated on coverslips were fixed in formaldehyde 4% and 0.2% glutaraldehyde for 15 min in a cold room. After three washes with PBS containing 50 mM NH_4Cl, the cells were incubated in buffer A (PIPES 20 mM pH 6.8, NaCl 137 mM, KCl 2.7 mM) containing 0.05% saponin, 5% NGS, 5% NHS and 50 mM NH_4Cl for 45 min on ice to reduce background staining. The coverslips were left overnight at 4°C in a humid chamber with the primary antibodies diluted in buffer A containing 0.1% saponin, 5% NGS and 5% NHS, then they were rinsed in buffer A and then

incubated for 3 h on ice with biotin-conjugated goat anti-mouse-IgM antibody diluted in buffer A containing 0.1% saponin, 5% NGS and 5% NHS. They were then rinsed in buffer A and then incubated in the dark for 1 h on ice in buffer A containing 0.1% saponin, 5% NGS and 5% NHS containing the secondary antibodies. Nuclei were stained with 5 µM Hoechst 33342 dye in 0.05 M Tris-HCl pH 7.4 for 2 min in the dark at room temperature. The specificity of PI(4,5)P2 staining was verified by the use of neomycin as reported by Hammond et al. (2006).

Microscope image acquisition

The slides were examined under a Zeiss AxioImager Z1 microscope (Zeiss, Oberkochen, Germany) equipped with a plan-Neofluar 40×0.75 NA (numerical aperture) dry objective and band-pass filters (set numbers 38, 15 and 49 for green, red and blue fluorochromes, respectively). Images (1388 by 1040 pixels) were acquired using a fixed exposure time with an AxioCam MRm (Zeiss) as 3×12 bit RGB proprietary zvi files (Zeiss), processed with AxioVision (4.6) software (Zeiss) and exported as 8-bit uncompressed TIF files. A Zeiss LSM780 confocal system fitted on an Observer Z1 inverted microscope equipped with alpha Plan-Apochromat 63×1.46 NA oil immersion objective (Zeiss, Iena, Germany) was used for confocal imaging. High-resolution confocal microscopy ideal sampling was calculated using a Nyquist calculator (Scientific Volume Imaging) for each objective. Images were acquired sequentially for each fluorochrome in the order infrared, red, green and blue, to avoid crosstalk. Resulting images were deconvoluted using Huygens Professional software (4.2; Scientific Volume Imaging). *Z*-planes containing structures of interest were projected into one picture, merged and presented as an interpolation display using ZEN 2010 D software (Carl Zeiss). For quantitative microscopy, images were taken under the same settings for both groups. Contrast was adjusted identically for all figures.

Fluorescence intensity quantification

Quantification was done using the Advanced Weka Segmentation plugin for ImageJ. Laser intensity and gain were set in the brightest sample below saturation, and this was kept during acquisition for both groups. Confocal images were deconvoluted and split into separate 16-bit TIF files. A binary mask was created and used to extract the mean pixel intensity at the plasma membrane per sample. Data were analyzed by Microsoft Excel software and plotted using Prism software (GraphPad).

Focal adhesion length measurement

pFAK Y397 as a focal adhesion marker and Hoechst 33342 was used for counterstaining. Three nonoverlapping fields were acquired on LSM780 confocal system from three different experiments. Counting was done in ImageJ (NIH). For length measurement, pFAK Y397 signals were measured using ZEN 2010 sofware.

Statistics

Data are mean±s.e.m.; they were analyzed by GraphPad Prism using two-way ANOVA followed by Bonferroni post-test for the scratch test and focal adhesion dynamics. For other data, we used a Student's *t*-test (two-tailed) followed by Mann–Whitney test. Statistical significance was defined as $P<0.05$. *$P<0.05$; **$P<0.01$; ***$P<0.001$; ****$P<0.0001$.

Acknowledgements

We are very grateful to Dr Marcelo Chavez for advice on immunocytochemistry of phosphoinositides, Mrs Catherine Valkeneers for preparing the primary cultures of glioblastoma, Mrs Colette Moreau for technical help, Dr Takeshi Nakamura for advice in shRNA transfection. We thank Dr Isabelle Salmon and Dr Peter Downes for providing the glioblastoma cell lines, Dr Tamas Balla for GFP-PH probes for monitoring phosphoinositides, and Dr Chris Mitchell for the GFP–SHIP2 construct.

Competing interests

The authors declare no competing or financial interests.

Author contributions

All authors contributed to the writing of the manuscript. W.E.E. performed most experimental work. J.-M.V. assisted W.E.E. in the immunofluorescence imaging work. R.D., V.J. and E.W. provided the proteomic analysis and S.G. the newly generated SHIP2 depleted glioblastoma cells. P.R. provided the primary cultures of human glioblastoma at the University of Liège. W.E.E. and C.E. were responsible for the design and the analysis of the experiments.

Funding

This work was supported by grants from the Fonds de la Recherche Scientifique Médicale (FRSM) [grant number PDRT.004.13 to C.E.] and by a grant of the Interuniversity Attraction Poles Programme (P6/28 and P7/13) Belgium State, Belgian Science Policy to C.E., V.J., R.D. and E.W. V.J., R.D. and E.W. were also supported by a G.O.A. grant [grant numbers GOA 08/016 and GOA 12/24] of the Flemish community. W.E.E. and S.G. are supported by Télévie fellowships (Belgium).

Supplementary information

Supplementary information available online at
http://jcs.biologists.org/lookup/suppl/doi:10.1242/jcs.179663/-/DC1

References

Balla, T. (2013). Phosphoinositides: tiny lipids with giant impact on cell regulation. *Physiol. Rev.* **93**, 1019-1137.

Ben-Chetrit, N., Chetrit, D., Russell, R., Korner, C., Mancini, M., Abdul-Hai, A., Itkin, T., Carvalho, S., Cohen-Dvashi, H., Koestler, W. J. et al. (2015). Synaptojanin 2 is a druggable mediator of metastasis and the gene is overexpressed and amplified in breast cancer. *Sci. Signal.* **8**, ra7.

Billcliff, P. G. and Lowe, M. (2014). Inositol lipid phosphatases in membrane trafficking and human disease. *Biochem. J.* **461**, 159-175.

Blero, D., De Smedt, F., Pesesse, X., Paternotte, N., Moreau, C., Payrastre, B. and Erneux, C. (2001). The SH2 domain containing inositol 5-phosphatase SHIP2 controls phosphatidylinositol 3,4,5-trisphosphate levels in CHO-IR cells stimulated by insulin. *Biochem. Biophys. Res. Commun.* **282**, 839-843.

Blero, D., Zhang, J., Pesesse, X., Payrastre, B., Dumont, J. E., Schurmans, S. and Erneux, C. (2005). Phosphatidylinositol 3,4,5-trisphosphate modulation in SHIP2-deficient mouse embryonic fibroblasts. *FEBS J.* **272**, 2512-2522.

Boucrot, E., Ferreira, A. P. A., Almeida-Souza, L., Debard, S., Vallis, Y., Howard, G., Bertot, L., Sauvonnet, N. and McMahon, H. T. (2015). Endophilin marks and controls a clathrin-independent endocytic pathway. *Nature* **517**, 460-465.

Chalhoub, N. and Baker, S. J. (2009). PTEN and the PI3-kinase pathway in cancer. *Annu. Rev. Pathol.* **4**, 127-150.

Choi, S., Thapa, N., Hedman, A. C., Li, Z., Sacks, D. B. and Anderson, R. A. (2013). IQGAP1 is a novel phosphatidylinositol 4,5 bisphosphate effector in regulation of directional cell migration. *EMBO J.* **32**, 2617-2630.

Choi, S., Thapa, N., Tan, X., Hedman, A. C. and Anderson, R. A. (2015). PIP kinases define PI4,5P(2) signaling specificity by association with effectors. *Biochim. Biophys. Acta* **1851**, 711-723.

Cunningham, D. L., Sweet, S. M. M., Cooper, H. J. and Heath, J. K. (2010). Differential phosphoproteomics of fibroblast growth factor signaling: identification of Src family kinase-mediated phosphorylation events. *J. Proteome Res.* **9**, 2317-2328.

Davies, E. M., Kong, A. M., Tan, A., Gurung, R., Sriratana, A., Bukczynska, P. E., Ooms, L. M., McLean, C. A., Tiganis, T. and Mitchell, C. A. (2014). Differential SKIP expression in PTEN-deficient glioblastoma regulates cellular proliferation and migration. *Oncogene* **34**, 3711-3727.

Deneubourg, L., Elong Edimo, W., Moreau, C., Vanderwinden, J.-M. and Erneux, C. (2014). Phosphorylated SHIP2 on Y1135 localizes at focal adhesions and at the mitotic spindle in cancer cell lines. *Cell Signal.* **26**, 1193-1203.

Dyson, J. M., O'Malley, C. J., Becanovic, J., Munday, A. D., Berndt, M. C., Coghill, I. D., Nandurkar, H. H., Ooms, L. M. and Mitchell, C. A. (2001). The SH2-containing inositol polyphosphate 5-phosphatase, SHIP-2, binds filamin and regulates submembraneous actin. *J. Cell Biol.* **155**, 1065-1080.

Elong Edimo, W., Derua, R., Janssens, V., Nakamura, T., Vanderwinden, J.-M., Waelkens, E. and Erneux, C. (2011). Evidence of SHIP2 Ser 132 phosphorylation, its nuclear localization and stability. *Biochem. J.* **439**, 391-401.

Elong Edimo, W., Vanderwinden, J. M. and Erneux, C. (2013). SHIP2 signalling at the plasma membrane, in the nucleus and at focal contacts. *Adv. Biol. Regul.* **53**, 28-37.

Erneux, C., Elong Edimo, W., Deneubourg, L. and Pirson, I. (2011). SHIP2 multiple functions: a balance between a negative control of PtdIns(3,4,5)P3 level, a positive control of PtdIns(3,4)P2 production, and intrinsic docking properties. *J. Cell Biochem.* **112**, 2203-2209.

Giuriato, S., Blero, D., Robaye, B., Bruyns, C., Payrastre, B. and Erneux, C. (2002). SHIP2 overexpression strongly reduces the proliferation rate of K562 erythroleukemia cell line. *Biochem. Biophys. Res. Commun.* **296**, 106-110.

Goni, G. M., Epifano, C., Boskovic, J., Camacho-Artacho, M., Zhou, J., Bronowska, A., Martin, M. T., Eck, M. J., Kremer, L., Grater, F. et al. (2014). Phosphatidylinositol 4,5-bisphosphate triggers activation of focal adhesion kinase by inducing clustering and conformational changes. *Proc. Natl. Acad. Sci. USA* **111**, E3177-E3186.

Hammond, G. R. V., Dove, S. K., Nicol, A., Pinxteren, J. A., Zicha, D. and Schiavo, G. (2006). Elimination of plasma membrane phosphatidylinositol (4,5)-

bisphosphate is required for exocytosis from mast cells. *J. Cell Sci.* **119**, 2084-2094.

Hammond, G. R. V., Schiavo, G. and Irvine, R. F. (2009). Immunocytochemical techniques reveal multiple, distinct cellular pools of PtdIns4P and PtdIns(4,5)P(2). *Biochem. J.* **422**, 23-35.

Hasegawa, J., Tokuda, E., Tenno, T., Tsujita, K., Sawai, H., Hiroaki, H., Takenawa, T. and Itoh, T. (2011). SH3YL1 regulates dorsal ruffle formation by a novel phosphoinositide-binding domain. *J. Cell Biol.* **193**, 901-916.

Ishihara, H., Sasaoka, T., Ishiki, M., Wada, T., Hori, H., Kagawa, S. and Kobayashi, M. (2002). Membrane localization of Src homology 2-containing inositol 5′-phosphatase 2 via Shc association is required for the negative regulation of insulin signaling in Rat1 fibroblasts overexpressing insulin receptors. *Mol. Endocrinol.* **16**, 2371-2381.

Kato, K., Yazawa, T., Taki, K., Mori, K., Wang, S., Nishioka, T., Hamaguchi, T., Itoh, T., Takenawa, T., Kataoka, C. et al. (2012). The inositol 5-phosphatase SHIP2 is an effector of RhoA and is involved in cell polarity and migration. *Mol. Biol. Cell* **23**, 2593-2604.

Kim, D.-H. and Wirtz, D. (2013). Focal adhesion size uniquely predicts cell migration. *FASEB J.* **27**, 1351-1361.

Kim, H. S., Li, A., Ahn, S., Song, H. and Zhang, W. (2014). Inositol Polyphosphate-5-Phosphatase F (INPP5F) inhibits STAT3 activity and suppresses gliomas tumorigenicity. *Sci. Rep.* **4**, 7330.

Krause, M. and Gautreau, A. (2014). Steering cell migration: lamellipodium dynamics and the regulation of directional persistence. *Nat. Rev. Mol. Cell Biol.* **15**, 577-590.

Ling, K., Doughman, R. L., Firestone, A. J., Bunce, M. W. and Anderson, R. A. (2002). Type I gamma phosphatidylinositol phosphate kinase targets and regulates focal adhesions. *Nature* **420**, 89-93.

McNulty, S., Powell, K., Erneux, C. and Kalman, D. (2011). The host phosphoinositide 5-phosphatase SHIP2 regulates dissemination of vaccinia virus. *J. Virol.* **85**, 7402-7410.

Muraille, E., Pesesse, X., Kuntz, C. and Erneux, C. (1999). Distribution of the src-homology-2-domain-containing inositol 5-phosphatase SHIP-2 in both non-haemopoietic and haemopoietic cells and possible involvement of SHIP-2 in negative signalling of B-cells. *Biochem. J.* **342**, 697-705.

Nakatsu, F., Perera, R. M., Lucast, L., Zoncu, R., Domin, J., Gertler, F. B., Toomre, D. and De Camilli, P. (2010). The inositol 5-phosphatase SHIP2 regulates endocytic clathrin-coated pit dynamics. *J. Cell Biol.* **190**, 307-315.

Onnockx, S., De Schutter, J., Blockmans, M., Xie, J., Jacobs, C., Vanderwinden, J.-M., Erneux, C. and Pirson, I. (2008). The association between the SH2-containing inositol polyphosphate 5-Phosphatase 2 (SHIP2) and the adaptor protein APS has an impact on biochemical properties of both partners. *J. Cell Physiol.* **214**, 260-272.

Ooms, L. M., Binge, L. C., Davies, E. M., Rahman, P., Conway, J. R., Gurung, R., Ferguson, D. T., Papa, A., Fedele, C. G., Vieusseux, J. L. et al. (2015). The inositol polyphosphate 5-phosphatase PIPP regulates AKT1-dependent breast cancer growth and metastasis. *Cancer Cell* **28**, 155-169.

Paternotte, N., Zhang, J., Vandenbroere, I., Backers, K., Blero, D., Kioka, N., Vanderwinden, J. M., Pirson, I. and Erneux, C. (2005). SHIP2 interaction with the cytoskeletal protein Vinexin. *FEBS J.* **272**, 6052-6066.

Pesesse, X., Dewaste, V., De Smedt, F., Laffargue, M., Giuriato, S., Moreau, C., Payrastre, B. and Erneux, C. (2001). The Src homology 2 domain containing inositol 5-phosphatase SHIP2 is recruited to the epidermal growth factor (EGF) receptor and dephosphorylates phosphatidylinositol 3,4,5-trisphosphate in EGF-stimulated COS-7 cells. *J. Biol. Chem.* **276**, 28348-28355.

Pirruccello, M. and De Camilli, P. (2012). Inositol 5-phosphatases: insights from the Lowe syndrome protein OCRL. *Trends Biochem. Sci.* **37**, 134-143.

Posor, Y., Eichhorn-Grünig, M. and Haucke, V. (2015). Phosphoinositides in endocytosis. *Biochim. Biophys. Acta* **1851**, 794-804.

Prasad, N., Topping, R. S. and Decker, S. J. (2002). Src family tyrosine kinases regulate adhesion-dependent tyrosine phosphorylation of 5′-inositol phosphatase SHIP2 during cell attachment and spreading on collagen I. *J. Cell Sci.* **115**, 3807-3815.

Prasad, N. K., Tandon, M., Badve, S., Snyder, P. W. and Nakshatri, H. (2008a). Phosphoinositol phosphatase SHIP2 promotes cancer development and metastasis coupled with alterations in EGF receptor turnover. *Carcinogenesis* **29**, 25-34.

Prasad, N. K., Tandon, M., Handa, A., Moore, G. E., Babbs, C. F., Snyder, P. W. and Bose, S. (2008b). High expression of obesity-linked phosphatase SHIP2 in invasive breast cancer correlates with reduced disease-free survival. *Tumour Biol.* **29**, 330-341.

Robe, P. A., Bentires-Alj, M., Bonif, M., Rogister, B., Deprez, M., Haddada, H., Khac, M.-T. N., Jolois, O., Erkmen, K., Merville, M. P. et al. (2004). In vitro and in vivo activity of the nuclear factor-kappaB inhibitor sulfasalazine in human glioblastomas. *Clin. Cancer Res.* **10**, 5595-5603.

Sharma, V. P., Eddy, R., Entenberg, D., Kai, M., Gertler, F. B. and Condeelis, J. (2013). Tks5 and SHIP2 regulate invadopodium maturation, but not initiation, in breast carcinoma cells. *Curr. Biol.* **23**, 2079-2089.

Song, M. S., Salmena, L. and Pandolfi, P. P. (2012). The functions and regulation of the PTEN tumour suppressor. *Nat. Rev. Mol. Cell Biol.* **13**, 283-296.

Sottoriva, A., Spiteri, I., Piccirillo, S. G. M., Touloumis, A., Collins, V. P., Marioni, J. C., Curtis, C., Watts, C. and Tavare, S. (2013). Intratumor heterogeneity in human glioblastoma reflects cancer evolutionary dynamics. *Proc. Natl. Acad. Sci. USA* **110**, 4009-4014.

Staiano, L., De Leo, M. G., Persico, M. and De Matteis, M. A. (2015). Mendelian disorders of PI metabolizing enzymes. *Biochim. Biophys. Acta* **1851**, 867-881.

Stauffer, T. P., Ahn, S. and Meyer, T. (1998). Receptor-induced transient reduction in plasma membrane PtdIns(4,5)P2 concentration monitored in living cells. *Curr. Biol.* **8**, 343-346.

Sun, Y., Thapa, N., Hedman, A. C. and Anderson, R. A. (2013). Phosphatidylinositol 4,5-bisphosphate: targeted production and signaling. *Bioessays* **35**, 513-522.

Takabayashi, T., Xie, M. J., Takeuchi, S., Kawasaki, M., Yagi, H., Okamoto, M., Tariqur, R. M., Malik, F., Kuroda, K., Kubota, C. et al. (2010). LL5beta directs the translocation of filamin A and SHIP2 to sites of phosphatidylinositol 3,4,5-triphosphate (PtdIns(3,4,5)P3) accumulation, and PtdIns(3,4,5)P3 localization is mutually modified by co-recruited SHIP2. *J. Biol. Chem.* **285**, 16155-16165.

Taylor, V., Wong, M., Brandts, C., Reilly, L., Dean, N. M., Cowsert, L. M., Moodie, S. and Stokoe, D. (2000). 5′ phospholipid phosphatase SHIP-2 causes protein kinase B inactivation and cell cycle arrest in glioblastoma cells. *Mol. Cell. Biol.* **20**, 6860-6871.

Tsujita, K. and Itoh, T. (2015). Phosphoinositides in the regulation of actin cortex and cell migration. *Biochim. Biophys. Acta* **1851**, 824-831.

Vandeput, F., Backers, K., Villeret, V., Pesesse, X. and Erneux, C. (2006). The influence of anionic lipids on SHIP2 phosphatidylinositol 3,4,5-trisphosphate 5-phosphatase activity. *Cell Signal.* **18**, 2193-2199.

Vandeput, F., Combettes, L., Mills, S. J., Backers, K., Wohlkonig, A., Parys, J. B., De Smedt, H., Missiaen, L., Dupont, G., Potter, B. V. et al. (2007). Biphenyl 2,3′,4,5′,6-pentakisphosphate, a novel inositol polyphosphate surrogate, modulates Ca2+ responses in rat hepatocytes. *FASEB J.* **21**, 1481-1491.

Venkatareddy, M., Cook, L., Abuarquob, K., Verma, R. and Garg, P. (2011). Nephrin regulates lamellipodia formation by assembling a protein complex that includes Ship2, filamin and lamellipodin. *PLoS. ONE* **6**, e28710.

Wang, Y. J., Keogh, R. J., Hunter, M. G., Mitchell, C. A., Frey, R. S., Javaid, K., Malik, A. B., Schurmans, S., Tridandapani, S. and Marsh, C. B. (2004). SHIP2 is recruited to the cell membrane upon macrophage colony-stimulating factor (M-CSF) stimulation and regulates M-CSF-induced signaling. *J. Immunol.* **173**, 6820-6830.

Westhoff, M. A., Karpel-Massler, G., Brühl, O., Enzenmüller, S., La Ferla-Brühl, K., Siegelin, M. D., Nonnenmacher, L. and Debatin, K.-M. (2014). A critical evaluation of PI3K inhibition in Glioblastoma and Neuroblastoma therapy. *Mol. Cell. Ther.* **2**, 32.

Wolfenson, H., Lavelin, I. and Geiger, B. (2013). Dynamic regulation of the structure and functions of integrin adhesions. *Dev. Cell* **24**, 447-458.

Xie, J., Vandenbroere, I. and Pirson, I. (2008). SHIP2 associates with intersectin and recruits it to the plasma membrane in response to EGF. *FEBS Lett.* **582**, 3011-3017.

Yu, J., Ryan, D. G., Getsios, S., Oliveira-Fernandes, M., Fatima, A. and Lavker, R. M. (2008). MicroRNA-184 antagonizes microRNA-205 to maintain SHIP2 levels in epithelia. *Proc. Natl. Acad. Sci. USA* **105**, 19300-19305.

Yu, J., Peng, H., Ruan, Q., Fatima, A., Getsios, S. and Lavker, R. M. (2010). MicroRNA-205 promotes keratinocyte migration via the lipid phosphatase SHIP2. *FASEB J.* **24**, 3950-3959.

Zaidel-Bar, R. and Geiger, B. (2010). The switchable integrin adhesome. *J. Cell Sci.* **123**, 1385-1388.